Influence of the flammable cloud geometry on the gas explosion effects

Jérôme Daubech, Jérôme Hebrard, Emmanuel Leprette

Influence of the flammable cloud geometry on the gas explosion effects

Jérôme Daubech[a], Jérôme Hebrard[a] & Emmanuel Leprette[a]

[a] Institut National de l'Environnement Industriel et des Risques, Parc Technologique ALATA, BP 2, 60550 Verneuil-en-Halatte, France

E-mail: jerome.daubech@ineris.fr

Abstract

In the context of industrial large cloud explosions such as the Buncefield accident (SCI, 2009), it is commonly accepted that the flammable cloud spreads over a large area on the ground but has a limited height. This can therefore be considered as the limiting dimension of the cloud. In this work at a small scale, Leyer (1982) highlights the influence of the limited height of the flammable cloud in the case of cylindrical cloud explosions. Without prejudging the combustion mechanisms, the objective of this paper is to present the influence of this limited dimension of the flammable cloud on the flame dynamics to assess more precisely the overpressure distances of a UVCE by a better determination of the energy involved in the explosion. The analysis is based on the comparison of the flame position over time from the fast video films and the overpressure signals recorded in the flammable clouds. The explosions examined are methane and hydrogen free jet (Sail, 2014; Daubech, 2015), methane jet interacting with the ground and rows of obstacles (Sail, 2014), and large propane clouds obstructed by rows of tree trunks (SCI, 2014).

Keywords: *UVCE, flammable cloud geometry, overpressure effects*

1. Introduction

The history of industrialization is punctuated by major unconfined explosions that have left their mark on the scale of the caused damage. The accidental sequence of this type of accident can be summarised as follows. An unconfined gas/vapor/air cloud is formed, its size, composition, and internal level of agitation (the "turbulence") depend on the type of leak that caused it. If an effective ignition source is introduced into the flammable area of the cloud, the cloud ignites and a flame starts to spread. In its path, the flame almost instantaneously transforms the cold reactants into very hot combustion products (from 1000 to 2000°C), which results in a strong volume expansion of the burnt gases. This volume expansion, which sets the atmosphere in motion like a piston (or a loudspeaker), is responsible for the pressure effects. In the open air and at a given distance from the explosion, the greater the expansion velocity of flame is, the greater the overpressure effects are. Among the well-known accidents, we can mention the UFA (Russia, 1989), Port Hudson (USA, 1970), more recently Buncefield (England, 2005), and Jaipur (India, 2009). All of the above accidents have the singularity that the flammable cloud spreads over a large area on the ground but has a limited height. For instance, an analysis of the Buncefield accident (SCI, 2009) shows that the winter-grade gasoline flammable cloud occupied an area of 120000 m^2 with a height of about 2 m. The Jaïpur gasoline cloud spreads over a radius of 350 m around the release point with a limited height giving a pancake shape to the flammable atmosphere (Oran, 2020). It appears that the flammable cloud has a much smaller characteristic size than the others.

One of the first to experimentally investigate the influence of flammable cloud geometry on the effects of an explosion was Leyer (1982). He has studied at the lab scale the pressure fields produced

by the explosion of a cylindrical cloud. Leyer extends the soap bubble technique of creating a hemispherical deflagration to cylindrical geometry. The soap films are held together by a cylindrical metal structure filled with an oxygen-doped ethylene-air mixture. This cylindrical volume is characterized by a radius R0 (9, 22 et 35 cm) and a height h_0 (2.4 cm ≤ h_0 ≤ 9 cm), which represents a volume between 0.6 to 17 liters. The flame dynamic is captured by a fast video camera (1500 frames/s) and a schlieren system. The overpressure is registered by microphone-type sensors. The analysis of fast video images shows a flame development in three successive steps.

The first step consists of a spherical development of flame until the burnt gases are allowed to escape toward the surroundings. The maximum radius r_{max} reached by the flame at the end of this spherical phase is given by the initial height of the cloud multiplied by the expansion ratio E raised to the power of one-third ($r_{max} = h_0.E^{1/3}$).

The second step is a radial propagation of the flame. The flame shape is a truncated hemisphere of nearly constant height which can be estimated as $h_0.E^{1/3}$. Above the flame front, an ascending convective motion of combustion products is observed. The flame propagation speed is slightly lower than in the first phase.

The last step is reached when the flame extends to the radial boundaries of the cloud which coincides with the end of combustion. The boundaries of the flammable cloud are materialized by the presence of a supporting ring which might be considered as an obstacle. The fast video images show that the ring induces a swirling motion of the outward expanding fresh mixtures. The flame front is considerably affected by this vortical structure inducing a strong flame area increase.

This dynamic flame development is visible on the pressure signal (Fig.1). The cylindrical pressure signal is compared to a hemispherical pressure signal with quite the same volume and the same flammable mixture (C_2H_4 + $3O_2$ + $12N_2$). Until 20 ms, the pressure rise-up is the same for the cylindrical and hemispherical volume. After, while the pressure continues to rise for the hemispherical cloud, the pressure reaches an almost constant plateau for the cylindrical cloud. For the cylindrical cloud, the end of the pressure signal is affected by a strong pressure peak which reflects the interaction of the flame front with the ring.

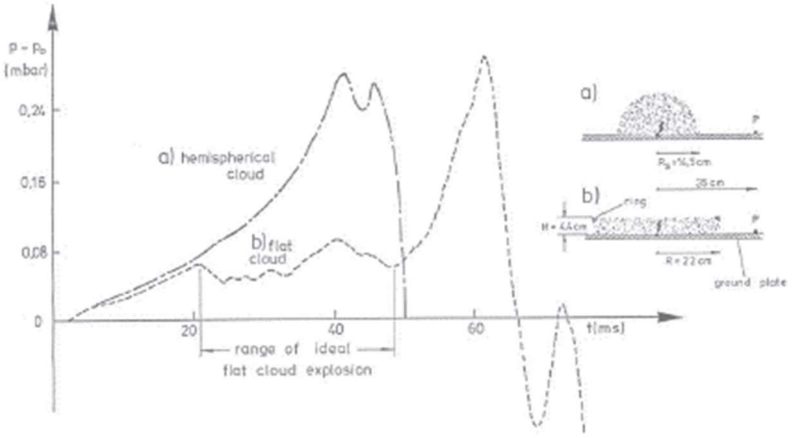

Fig. 1. Pressure signals (Leyer, 1982) obtained in soap bubble experiments from the explosion of a hemispherical cloud and of a flat cloud of equal volume (a – hemispherical cloud – Radius = 14.5 cm – Volume: 6385 cm³ / b – cylindrical cloud – Radius = 22.5 cm, height = 4.4 cm – Volume = 6690 cm³)

This pressure signal compared with a spherical cloud underlines the role of the flammable cloud geometry and more particularly the limited dimension (height of cloud) on the overpressure pressure and the flame dynamic.

The objective of this paper is to present the influence of this limited dimension of the flammable cloud on the flame dynamics and the overpressure effects by an analysis of several explosion configurations at intermediate or large scales like:

- methane and hydrogen free jet explosion (Sail, 2014; Daubech, 2015),
- methane jet interacting with the ground and rows of obstacles (Sail, 2014),
- large propane clouds obstructed by rows of tree trunks (SCI, 2014).

The analysis is based on the comparison of the flame position versus time from the fast video films and the overpressure signals recorded in the flammable clouds.

2. Flame dynamics and overpressure effects

The purpose of this section is to describe the experimental bench which provided experimental data to allow us to evaluate the influence of a flammable cloud limited dimension on flame dynamics and associated overpressure effects in several experimental configurations of UVCE.

2.1 Methane and hydrogen free jet explosion

The same experimental installation is used for methane and hydrogen jet release and jet explosion. Sail (2014) and Daubech (2015) present in detail the experimental setup. The release was produced by a 12 mm diameter orifice fuelled by a 5 m^3 tank (Fig.2). The tank is filled with methane or hydrogen initially pressurized at 40 bar. This configuration ensures a low decrease of the 5 m^3 tank pressure and a low decrease of the mass release rate during the tests (only a few seconds for jet explosion tests).

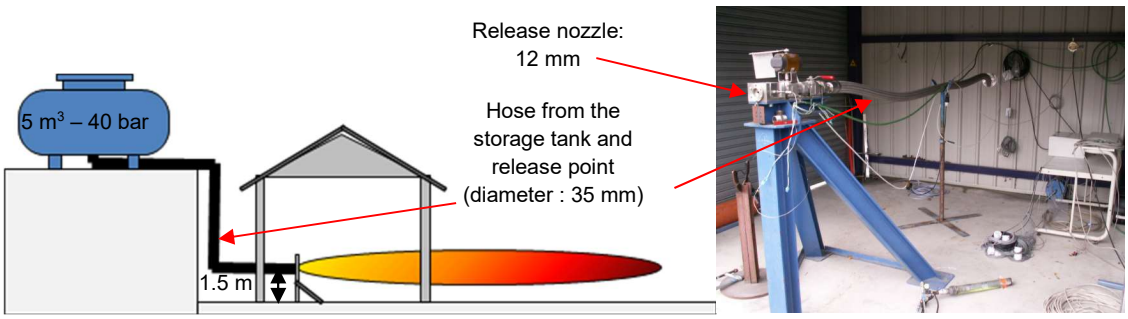

Fig. 2. Scheme of experimental device and release point

The ignition source is a vertical steel tube (diameter: 5.5 cm – length: 50 cm) filled with an H2/O2 stoichiometric mixture ignited by a pyrotechnical match (60 J). The measurement of overpressure is performed using 3 piezoresistive pressure sensors Kistler 0-2 bar. These sensors are embedded in lens support which allows the measurement of incident pressure waves without any reflection effect. Fig. 3 presents the overall repartition of pressure gauges. The flame dynamic is captured by image processing from fast videos. The image processing is the BOS method. A reference image is subtracted from the image sequence. To obtain more detail on the burnt gas pocket, the greyscale of each pixel is multiplied by 10. A Boolean rule is applied to keep the pixel above a specifically defined grayscale level for each test. The value of pixel grayscale is changed to 255 for pixels above de specific grayscale level and 1 for the others.

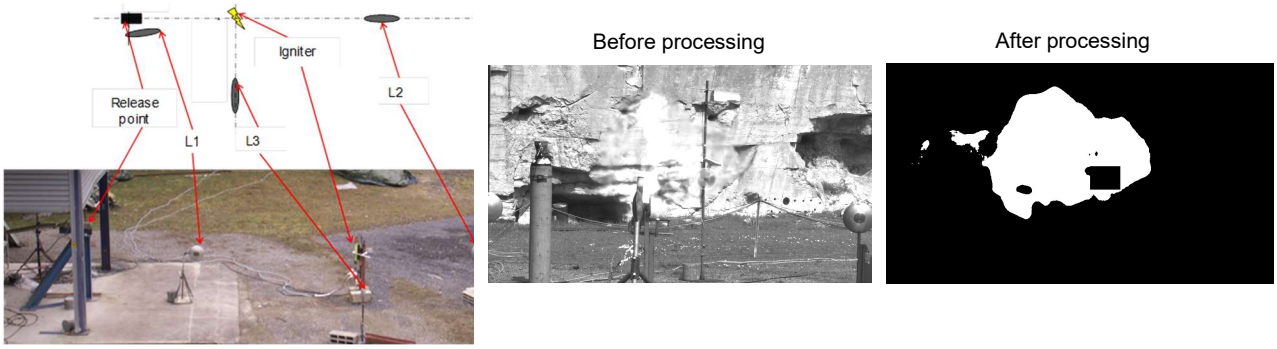

Fig. 3. Overall repartition of pressure gauges and flame image processing

For methane jet explosion, the chosen explosion configuration is for an ignition realized at a concentration of around 13 % (Sail, 2014). The axial lower flammability limit (LFL) distance is around 5.5 m from the release point and the maximal radial LFL distance is around 0.4 m from the axis of the jet. Fig.4 presents the pressure signal registered by the L3 gauge sensor located at 3 m from the ignition source, flame position, and flame velocity deduced from the fast video. The flame velocity in four directions (upstream, downstream, upwards, and downwards from ignition) is presented versus time and distance from the ignition source.

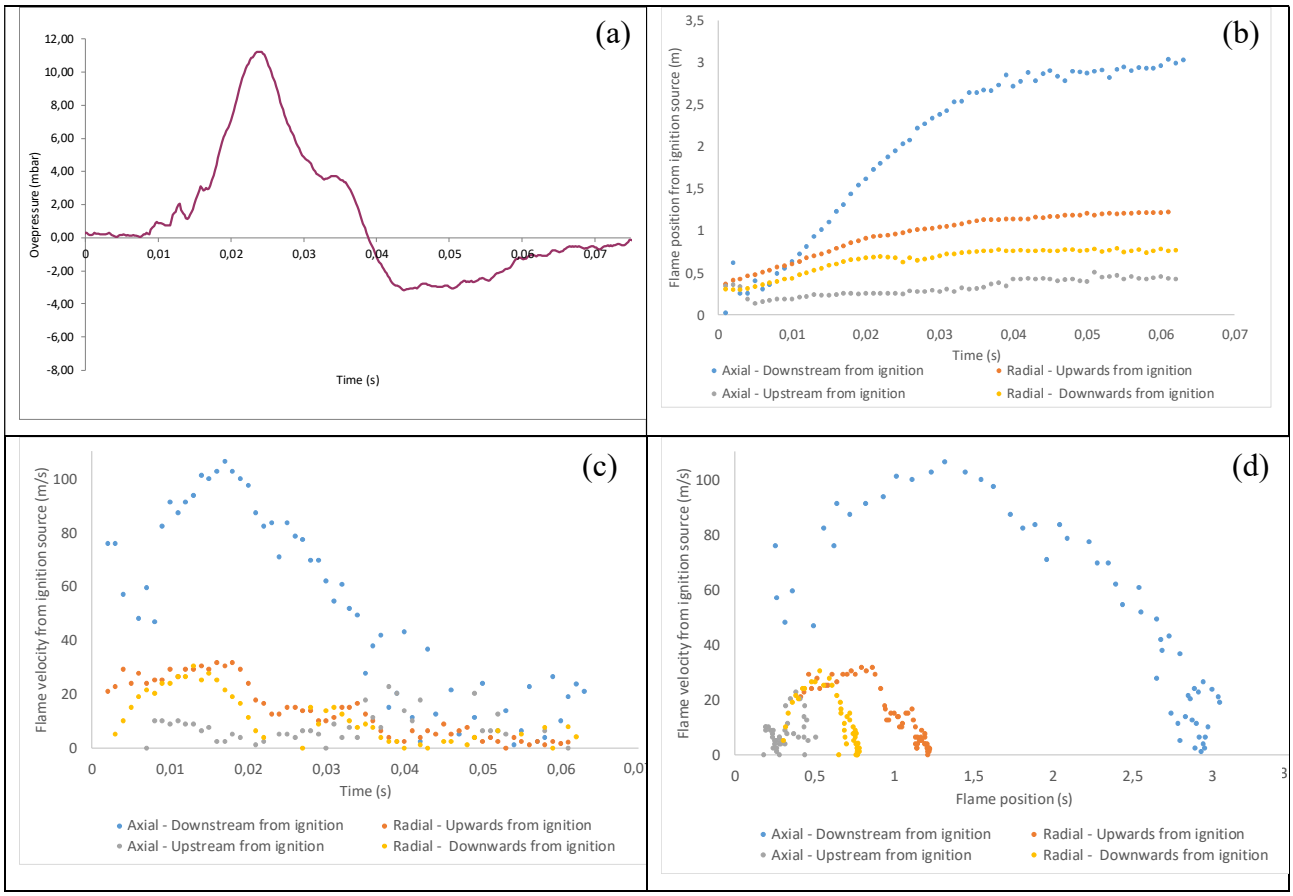

Fig. 4. Pressure signal registered by L3 gauge sensor located at 3 m from ignition source (a), the flame position (b) and flame velocity(c), and flame velocity versus flame position (d) deduced from the fast video movie

The maximum overpressure registered at 3 m from ignition is around 12 mbar and occurs at 23 ms. Radial upwards and axial downstream flame velocities are maximum at 18 ms, respectively around 30 m/s and 105 m/s (figure 4c). After 18 ms, the flame velocities decrease. When both velocities are maximum, the downstream flame position is around 1.35 m and the upward flame position is around 0.85 m (figure 4d).

The time between the flame velocity and overpressure peak is 5 ms. If we consider that pressure waves propagate at the speed of sound (340 m/s), the distance traveled by a pressure wave in 5 ms is 1.7 m, i.e. *ca.* the distance from the flame to the sensor, thus pressure peak might occur when the flame velocities are maximum. But, when flame velocity is maximum, the radial flame position is 0.85 m, which corresponds approximately to the maximum flame radius calculated by Leyer at the end of spherical flame propagation for a cylindrical cloud1 ($r_{max} = h_0 \times E^{1/3}$). It seems also to show that the overpressure peak occurs when the flame reaches the radial boundary of the flammable cloud whereas the downstream flame propagation is still possible (LFL distance = 5.5 m). Thus, the overpressure effects develop when the flame is fully subjected to thermal expansion. When the burnt

[1] Here, $h_0 = 0.45$ m and $E \approx 7.5$.

gas pocket is punctured as the flame reaches the cloud boundary, the flame speed decreases sharply. So, It also implies that only one part of the cloud is involved in the overpressure effects.

For hydrogen jet explosion, Daubech (2015) presents in detail the experimental set-up and the experimental work on hydrogen dispersion. This work shows that, for an initial tank pressure of 40 bar through a 12 mm hole, the axial LFL distance is around 20 m. The same release setup is used (replacing methane with hydrogen). The two main differences between methane and hydrogen configurations are ignition (100 mJ spark instead of 60J) and the pressure sensors' positions (see Fig. 5). The ignition occurs at 0,8 m from the release hole where the concentration is 50 % of H2 in air and the radial LFL distance is around 0,2 m from the jet axis. As sensor L1 is located right next to the ignition source, all the overpressure history is registered by this gauge.

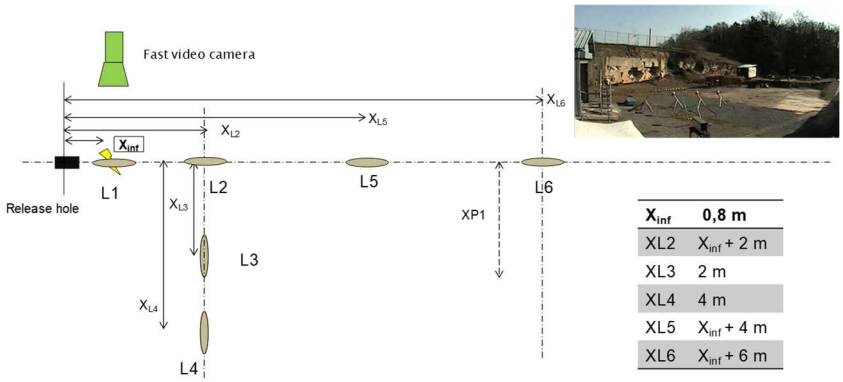

X_{inf}	0,8 m
XL2	X_{inf} + 2 m
XL3	2 m
XL4	4 m
XL5	X_{inf} + 4 m
XL6	X_{inf} + 6 m

Fig. 5. Overall repartition of pressure gauges

Fig.6 presents the pressure signal registered by L1 and L2 sensors, the flame position, and flame velocity deduced from the fast video movie. The flame velocity in four directions (upstream, downstream, upwards, and downwards from ignition) is presented versus time and versus distance from the ignition source.

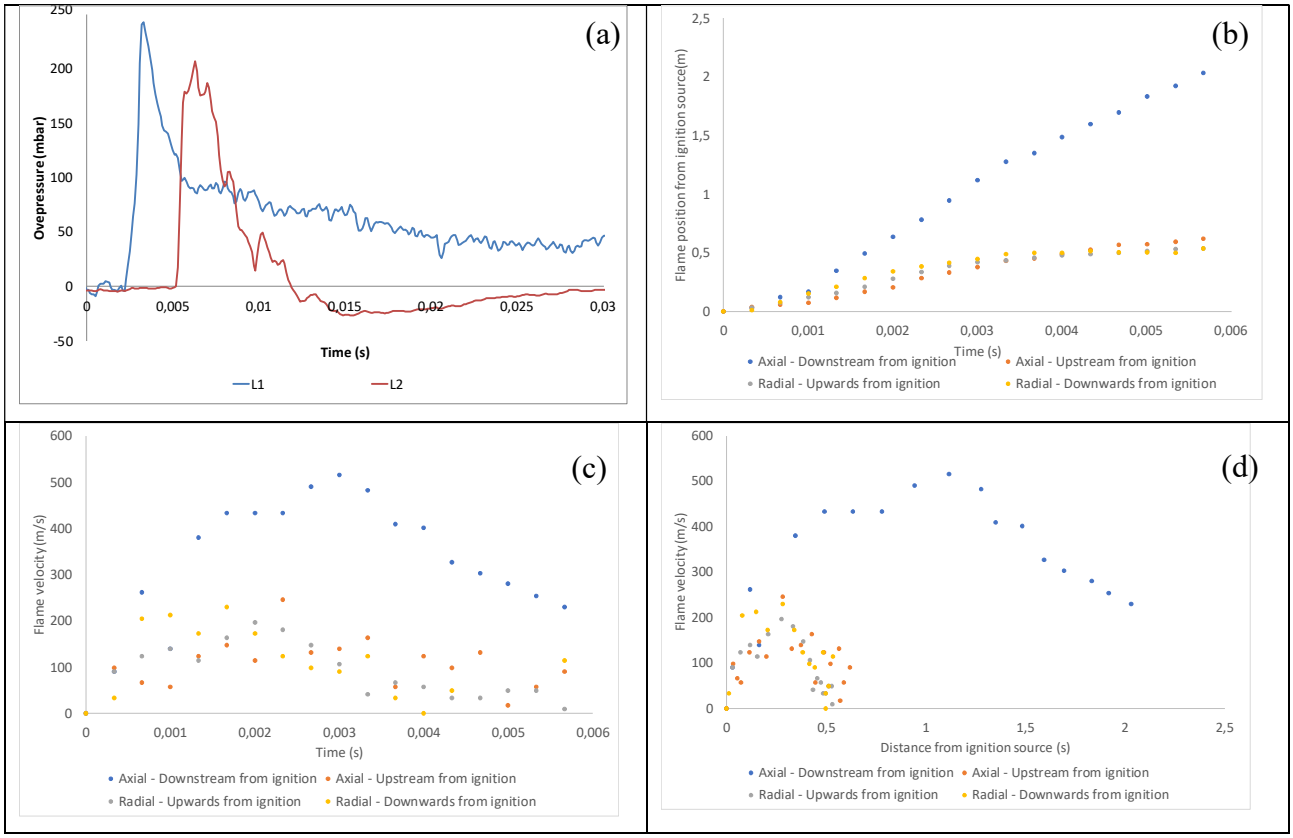

Fig. 6. Pressure signal registered by L1 and L2 gauge sensor (a), the flame position (b) and flame velocity(c), and flame velocity versus flame position (d) deduced from the fast video movie

The maximum overpressure is around 240 mbar and occurs at 3 ms. If we focus on flame dynamics, we notice that the radial and the axial downstream flame velocities are maximum at 3 ms, respectively around 200 m/s and 450 m/s. After 3 ms, the flame velocities decrease. When the velocities are maximum, the downstream flame position is around 1.2 m and the upward flame position is around 0.35 m.

As previously presented for methane jet explosion, this test confirms that the overpressure peak occurs when the flame velocities are maximum. The flame velocities are maximum when the radial position is around 0,35 m, which has also the same order of magnitude as the maximum flame radius calculated by Leyer at the end of spherical flame propagation[2] ($r_{max} = 0{,}2 \times (5{,}4)^{1/3}$). Even with a more reactive gas, the overpressure peak seems also occurs when the flame reaches the radial boundary of the flammable cloud where the flame is fully subjected to thermal expansion. After, the flame velocity and the overpressure decrease. Here, only a small part of the cloud is involved in the overpressure effects.

2.2 Methane jet interacting with the ground and rows of obstacles

The following configuration has been already presented by Sail (2014). This is a methane release under an initial pressure of 40 bar through a 12 mm circular orifice. The release is horizontal at 25 cm from the ground. The flammable cloud that is formed interacts with a wire mesh of welded 2 cm tube 30 cm high, 3 m long, and 1 m wide (Fig.7). The ignition of this flammable cloud is achieved using a pyrotechnic match (60 J) located in a 10 cm high, 15 cm long, and 12 cm deep containment with an open wall directed towards the axis of the release (Fig.7). The containment is filled with a flammable mixture. A flame of about ten centimeters in diameter ignites the external flammable cloud.

Fig. 7. Experimental configuration and ignition box

The pressure instrumentation shown in Fig. 8 consists of 6 pressure sensors, 3 of which are located in the wire mesh at 0.3 m (L3), 1 m (L5), and 2.1 m from the igniter. Two high-speed cameras film the explosion to capture the flame trajectory. Two pressure sensors are located outside the wire mesh: sensor L6 at 1 m from the end of the wire mesh and sensor L7 at 2.5 m from the axis of the discharge aligned with sensor L4.

The dispersion study in this configuration (Sail, 2014) shows that the wire mesh is filled with a stoichiometric methane/air mixture.

[2] Here , $h_0 = 0.2$ m and $E \approx 5.4$

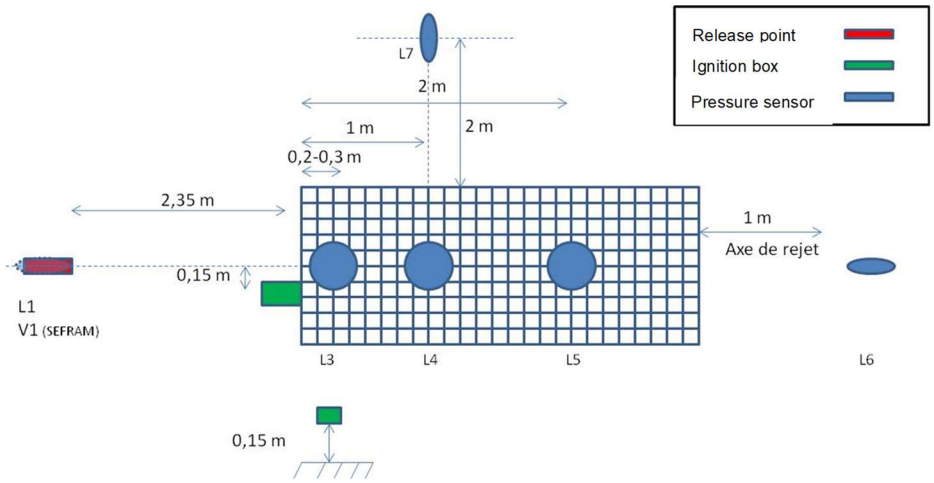

Fig. 8. Instrumentation

Fig.9 presents the pressure signal registered by L1 and L2 sensors, the flame position, and flame velocity deduced from the fast video movie. The flame velocity in four directions (upstream, downstream, upwards, and downwards from ignition) is presented versus time and distance from the ignition source.

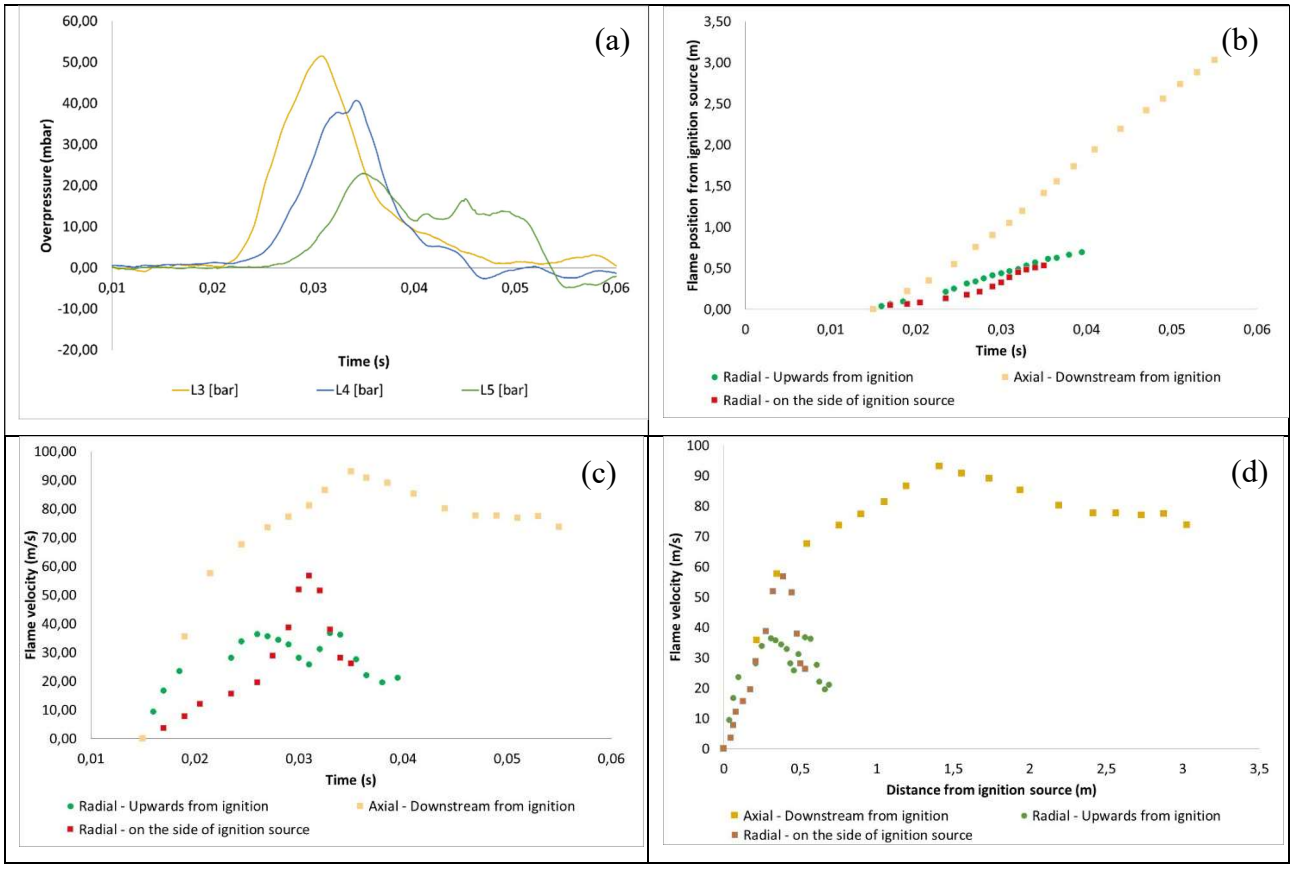

Fig. 9 Pressure signal registered by L3, L4, and L5 gauge sensors (a), the flame position (b) and flame velocity(c), and flame velocity versus flame position (d) deduced from the fast video movie

The flame travels axially 1.1 m, vertically 50 cm, and radially 40 cm when the peak of the overpressure is reached at 31 ms. Only a small part of the cloud burned at the time of the overpressure peak. If we analyze the evolution of the flame velocities in a little more detail, we can see that :

- when the flame reaches vertically 30 cm, i.e. when it reaches vertically the upper limit of the cluttered area, the flame slows down, passes through a minimum at 46 cm, re-accelerates before waiting for the upper limit of the cloud, and goes out when the flame reaches 60 cm, i.e. twice the height of the cloud (as observed earlier). This re-acceleration of the flame causes an increase in velocity on the axial velocity and a slight increase in pressure visible on the L4 sensor signal,
- When the flame reaches 40 cm radially, i.e. when it reaches the edge of the clogged area radially, the flame slows down,
- When the flame reaches 1.5 m axially, the flame velocity decreases and propagates at a constant speed. This directly impacts the pressure signal, where the pressure becomes constant at around 15 mbar (sensor L5).

2.3 Large propane clouds obstructed by rows of tree trunks

These tests were realized (SCI, 2014) by DNV GL on the experimental site of Spadeadam (UK). The objectives of these large-scale experiments are to study the different parameters that influence the acceleration of flames in vegetation: length, width, density, and type of vegetation and to verify that the transition to detonation is possible in a hedge (unconfined and very crowded environment). The stoichiometric propane/air mixture was contained in a tarpaulin-covered metal structure (Fig.10) whose length varies from 51 to 120 m depending on the experimental configurations. The width of the metallic structure is 4,5 m and its height is 3 m. Tarpaulin is cut by a pyrotechnic device just before ignition The congested areas are shorter than the total length of the cloud. Trees used for congestion are spruce, alder, and birch. The ignition is realized by a spark generator located on the centreline of the tree row at 1 m from the congested area edge and at 100 mm from ground level.

Fig. 10. Tarpaulin-covered metal structure and example of congestion

The overpressure is measured by piezo-electric pressure transducers deployed inside and outside the flammable cloud. Twelves pressure sensors are spaced 3 m apart on the axis of the ignition cloud at 1.75 m. Flame arrival time was measured through the test rig using an array of ionization probes located at the same position as pressure sensors.
Video footage from each experiment was recorded using both high-speed and normal-speed digital video cameras.

It is chosen here to present and compare two tests (3 and 4) carried out under similar conditions. In both cases, the dimensions of the flammable cloud are 51 m x 4.5 m x 3 m, and the dimensions of the congested area are 30 m x 4.5 m x 3 m. The difference between the two tests comes from the nature of the congestion. The congestion of test 3 consists of alders with 2 trees/m^2 and 15 fence posts of 8" on the center separated by 2 m. The congestion of test 4 is alder with 1.5 trees/m^2.

Test 3 remained in deflagration while Test 4 led to a deflagration detonation transition. The difference between the two explosion dynamics comes from the difference in the congestion. The congestion analysis by DNV GL shows that the average surface blockage rate is similar in both cases and the volume blockage rate in test 3 is 1.5 times higher than in test 4. However, the analysis shows that the density of small diameter obstacles is greater in Test 4 than in Test 3, which would have favored the acceleration of the flame and the deflagration-detonation transition.

Let us analyze the dynamics of the development of the flame in more detail thanks to the fast videos. The analysis of the videos is less precise than those carried out previously because of the dimensions of the experiment. However, it allows us to draw the main trends. The Fig.11. presents the pressure signals registered by P1 to P6 located between 3 and 18 m from the ignition source (SCI, 2014), the flame position, and flame velocity deduced from the fast video movie for Test 3. Fig.12 presents the same data for Test 4.

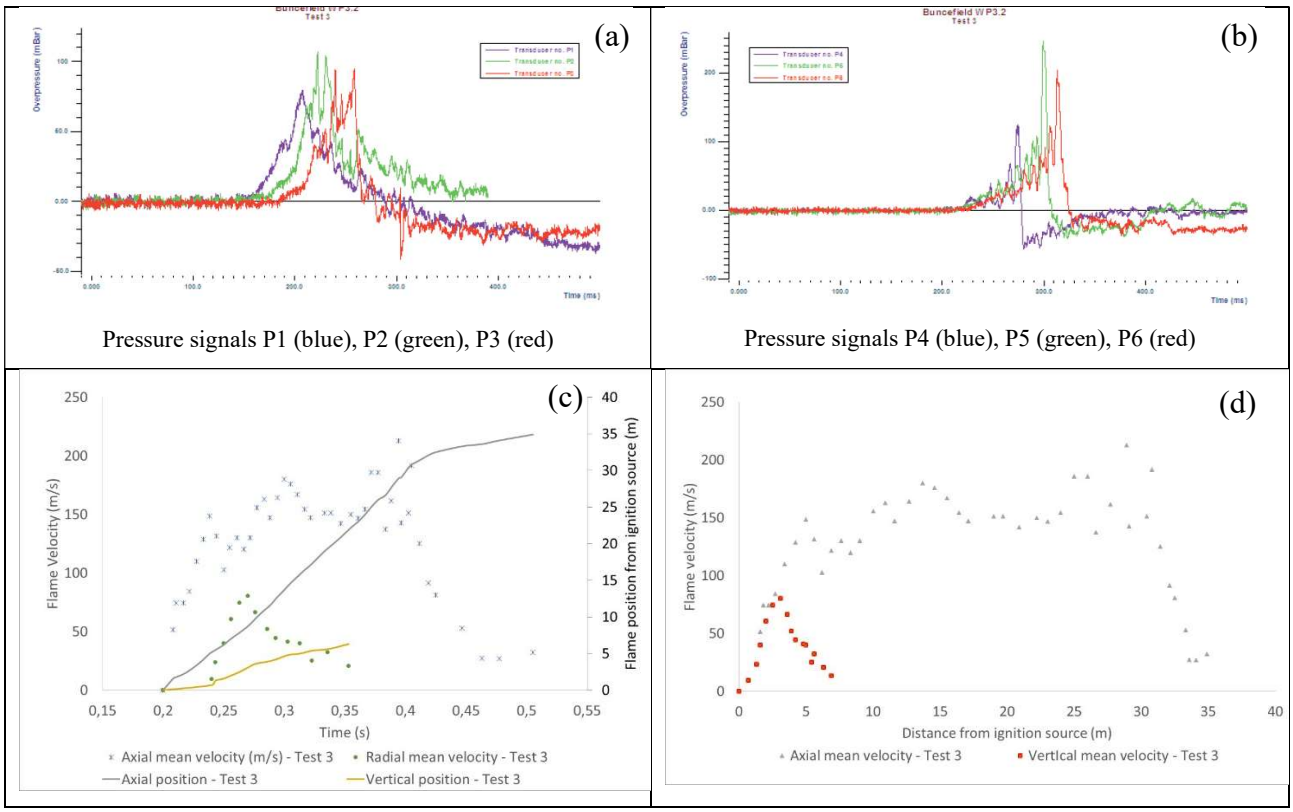

Fig. 11. Test 3 - Pressure signals registered by P1 to P6 gauge sensors located between 3 and 18 m from ignition source (a-b), the flame position and flame velocity(c), and flame velocity versus flame position (d) deduced from the fast video movie

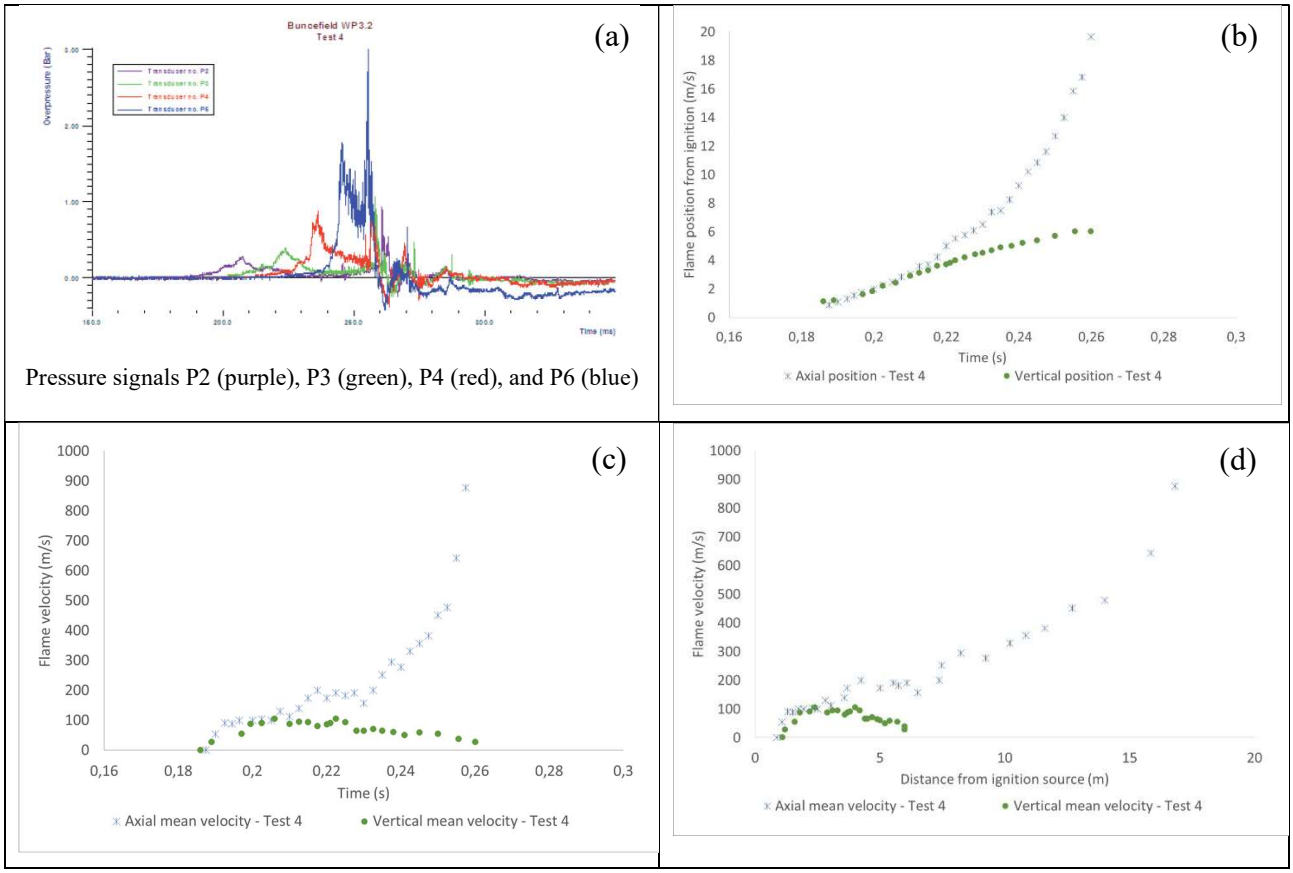

Fig. 12. Test 4 - Pressure signal registered by P2 to P6 gauge sensors located between 6 and 18 m from ignition source (a), the flame position (b) and flame velocity(c), and flame velocity versus flame position (d) deduced from the fast video movie

For test 3, the maximum overpressure is recorded at 245 mbar at sensor 5 located 15 m from the ignition source. At 15 m the flame reaches a peak speed of around 180 m/s. At this point, the flame is located vertically at 5.5 m, i.e. about twice the distance between the ignition source and the initial position of the top of the cloud. This corresponds to the height that could be calculated with the Leyer relation used previously. Afterward, the flame slows down and seems to propagate at a constant speed of about 150 m/s until it reaches the end of the cluttered area at 30 m. In this zone, a quasi-constant pressure of about 100 mbar is established (SCI, 2014). After 30 m, the flame speed drops significantly to around 25 m/s. It can therefore be seen that when the flame reaches the upper boundary of the cloud, the axial flame propagation velocity and the overpressure are at their maximum. Afterward, the flame slows down to a constant speed. This flame behavior is similar to the one presented in the previous experimental configuration.

For Test 4, it appears that the deflagration-detonation transition occurs around a distance of the order of 15 m where the flame speed reaches 500 m/s. The pressure sensors P4 and P6 show this deflagration detonation transition with the appearance of a steep pressure front between 240 and 250 ms. At this moment, the flame altitude is about 5.5 m, the maximum vertical flame propagation height (Leyer relation). This shows that the deflagration-detonation transition occurs when the flame is still fully subjected to the thermal expansion of the burnt gases.

3. Discussion

Analysis of the flame propagation dynamics and pressure signals of the experimental set-ups presented above shows the impact of the limiting dimension of the flammable cloud. When the flame reaches the cloud boundaries, the flame velocity is maximal in the case where a deflagration

detonation transition does not occur. The pressure peak occurs at this point. Then the flame slows down, and the pressure drops to a constant value.

We can wonder what the impact of these flame dynamics on the pressure effects outside the cloud is. For this purpose, we try to reconstruct the pressure signals ΔP at the distance r thanks to the acoustic source model of Leyer (1982):

$$\Delta P(\tau, r) = \rho_0 . \frac{(1 - E^{-1})}{4.\pi.r} . \frac{\partial^2 V_{BG}}{\partial \tau^2}$$

With $\tau = t + \frac{r - r_f}{c}$

V_{BG} is the volume of burnt gases, r_f is the flame position, r is the target position and c is the speed of sound.

The flame path diagram makes it possible to reconstruct the volume of burnt gases. Thus, the volume change of the acoustic source is known.

First, this exercise is made on the hydrogen jet explosion regarding the pressure signal registered at 4 m from the axis of the release (Fig. 5). Fig. 13 presents a comparison between the estimated and experimental signals and the evolution of burnt gas volume. There is good agreement on both the shape and amplitude of the estimated pressure signal. The overpressure peak occurs at 15 ms, which corresponds to a time of 3 ms without the time lag due to the propagation of the pressure wave. At this moment, the volume of burnt gases is around 0,6 m^3, the flame velocity is maximum. As mentioned earlier, it coincides with the moment when the flame reaches the radial boundary of the flammable cloud. Considering a mean expansion ratio of burnt gas equal to 5,4, the volume of fresh gases implies in the explosion effects is around 0,1 m^3, whereas the total flammable volume above the LFL is around 40 m^3. Thus, only a small part of the flammable cloud participates in the overpressure effects at distance.

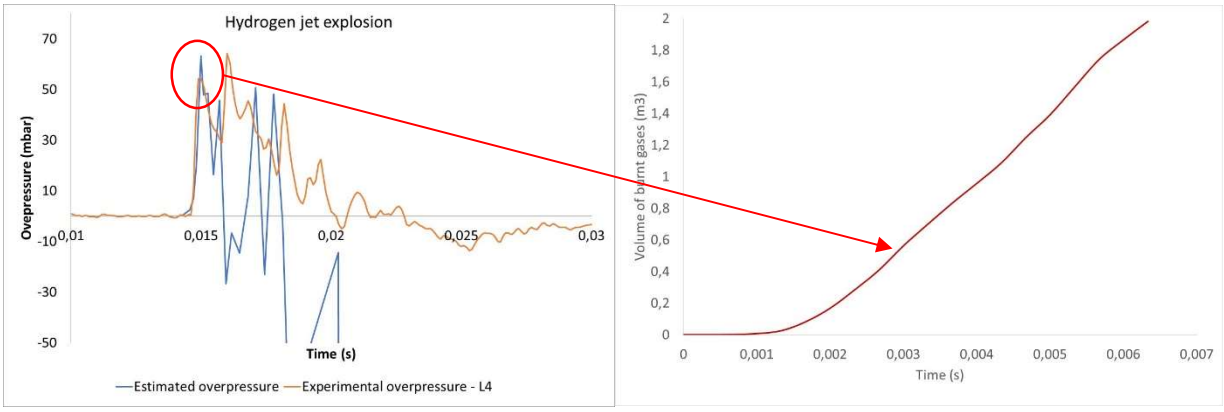

Fig. 13. Estimated and the experimental L4 pressure signals of hydrogen jet explosion and evolution of burnt gases volume

The same approach is made to the Methane jet explosion interacting with the ground and rows of obstacles. The reference pressure signal is the L6 sensor registered at 4 m from the ignition source on the axis of the release (Fig. 8). Fig. 14 presents a comparison between the estimated and the experimental signals and the evolution of burnt gases volume. There is also good agreement on both the shape and amplitude of the estimated pressure signal. The overpressure peak occurs at 45 ms, which corresponds to a time of 34 ms without the time lag due to the propagation of the pressure wave. At this moment, the volume of burnt gases is around 0.5 m^3. With a mean expansion ratio of burnt gas of about 6.4, the volume of fresh gases implies in the explosion effects is around 0,08 m^3, whereas the total flammable volume above the LFL is around 0.9 m^3. Thus, this shows again that only a small part of the flammable cloud participates in the overpressure effects at distance.

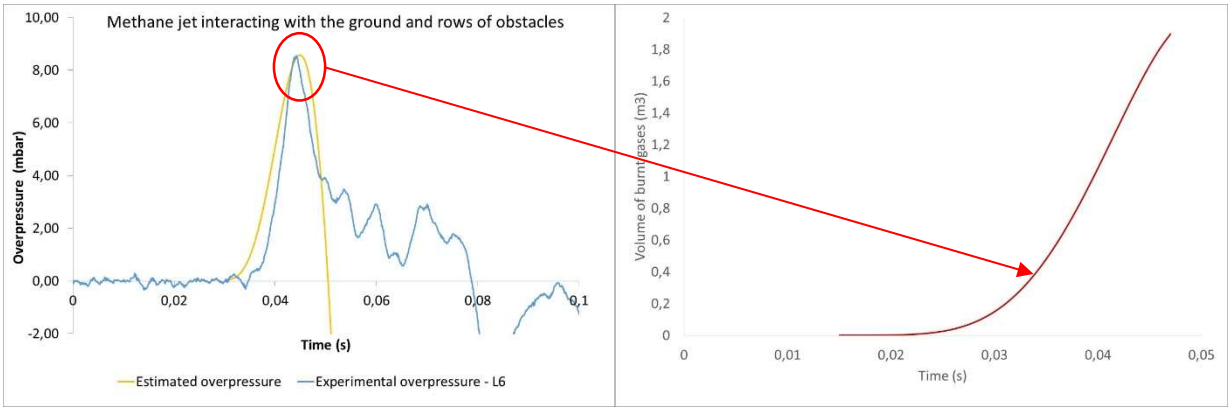

Fig. 14. Estimated and the experimental L6 pressure signals of hydrogen jet explosion interaction with the ground and obstacles and evolution of burnt gases volume

4. Conclusions

Flame dynamics analysis shows that when the flame reaches the cloud boundary (generally the smallest of the characteristic dimensions of the flammable cloud), the flame speed is at its maximum. It is at this point that the peak overpressure occurs. Then, when the pocket of burnt gases bounded by the flame is punctured, the burnt gases escape and the flame slows down to a constant speed if the mixture is homogeneous. It appears that the pressure is constant in the area where the flame propagates at a constant speed. If a deflagration-detonation transition occurs, it appears to occur when the flame is fully subjected to the thermal expansion of its combustion products. Large-scale tests would be interesting to see if turbulent and obstructing conditions can lead to a deflagration-detonation transition when the flame is no longer subject to its volume expansion, as in the case of Test 3 of the SCI tests.

The analysis of the pressure signals that can be made about the evolution of the volume of the burnt gas pocket shows that a part of the flammable cloud participates in the overpressure effects. This has direct consequences on the evaluation of the combustion energy involved in an explosion and on the calculation of the overpressure effect distances that could be estimated using the multi-energy method, for example.

References

Steel Construction Institute (2009). Buncefield Explosion Mechanism Phase 1 - Volume 1.

Oran E, Chamberlain G, Pekalski A, (2020), Mechanisms and occurrence of detonations in vapor cloud explosions, Progress in Energy and Combustion Science, vol 77, 100804

Leyer J.C (1982) An Experimental Study of Pressure Fields by Exploding Cylindrical Clouds, Combustion and flame, vol 48, pp 251-263

Sail J, Blanchetiere V, Geniaut G, Osman K, Daubech J, Jamois D, Hebrard J. (2014). Review of knowledge and recent works on the influence of initial turbulence in methane explosion. Proceeding of X. ISHPMIE, Bergen, Norway.

Daubech J, Hebrard J, Jallais S. Vyazmina E, Jamois D, Verbecke F, (2015), Un-ignited and ignited high pressure hydrogen releases: Concentration – turbulence mapping and overpressure effects, Journal of Loss Prevention in the Process Industries Volume 36, July 2015, Pages 439-446

Steel Construction Institute (2014). Dispersion and Explosion Characteristics of Large Vapour Clouds Volume 1 – Summary Report